Electronic supplementary information

Stabilizing Cathodes of Lithium-Sulfur Battery by Chemical Binding of Sulfur and Their Discharge Products to Carbon Nanofibers

Dan Li, Jie Liu, Na Xu, Mengfan Wang, Xuejun Liu, Tingzhou Yang, Tao Qian, Chenglin Yan*

College of Energy, Key Laboratory of Advanced Carbon Materials and Wearable Energy Technologies of Jiangsu Province, Soochow University, Suzhou 215006, China.

*Corresponding author: tqian@suda.edu.cn

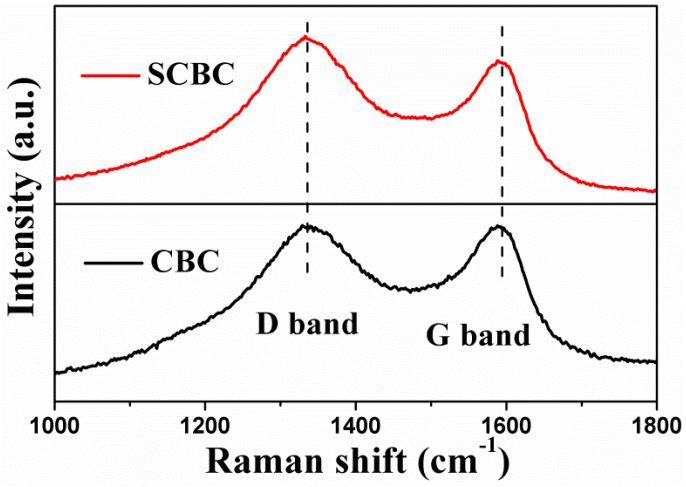

Fig. S1 The comparison of SCBC and carbonized bacterial cellulose in Raman spectra, manifesting the successful graft of sulfydryl groups on carbonized bacterial cellulose.

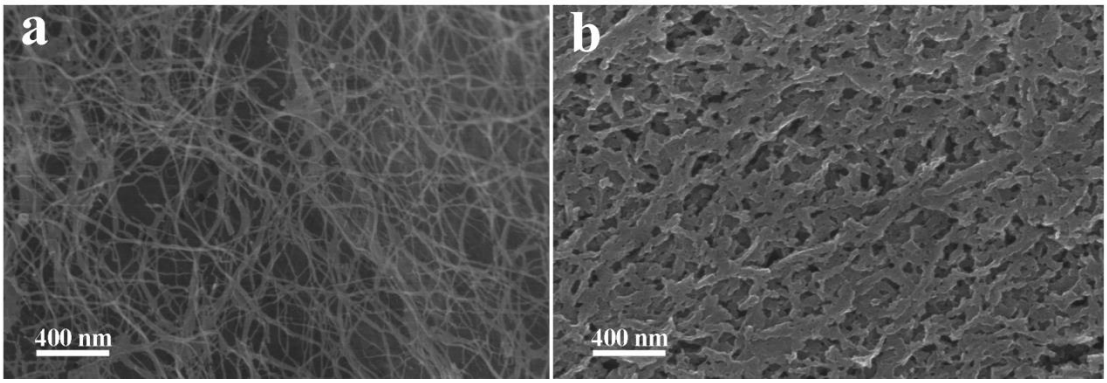

Fig. S2 SEM images of (a) carbonized bacterial cellulose and (b) SCBC nanofiber.

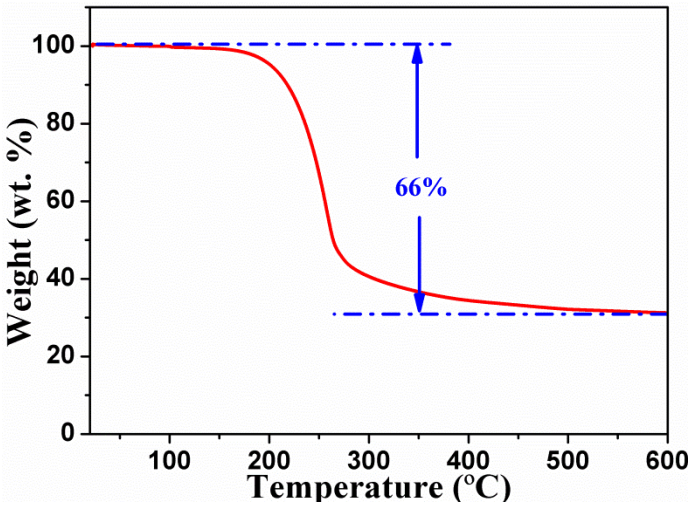

Fig. S3 TGA profiles for SCBC/S from 25 to 500 ℃ at a rate of 10 ℃ min^{-1}, the total content of sulfur in SCBC/S is ~66%.

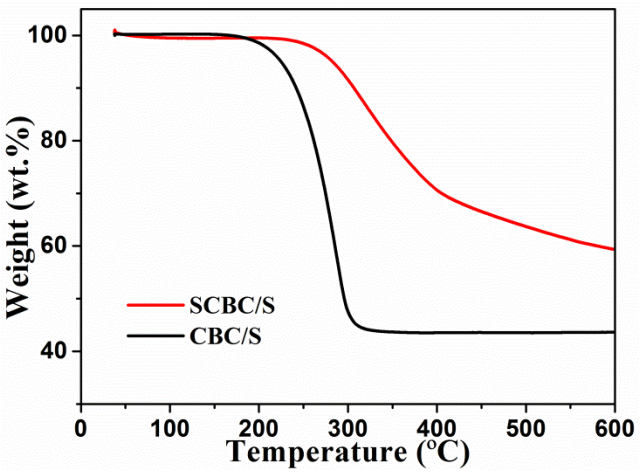

Fig. S4 TGA comparison. After removing sulfur inside the matrix physically completely, sulfur in SCBC/S exhibited a higher decomposition temperature (>245 ℃) than CBC/S, demonstrating small sulfur molecules are covalently bound to SCBC.

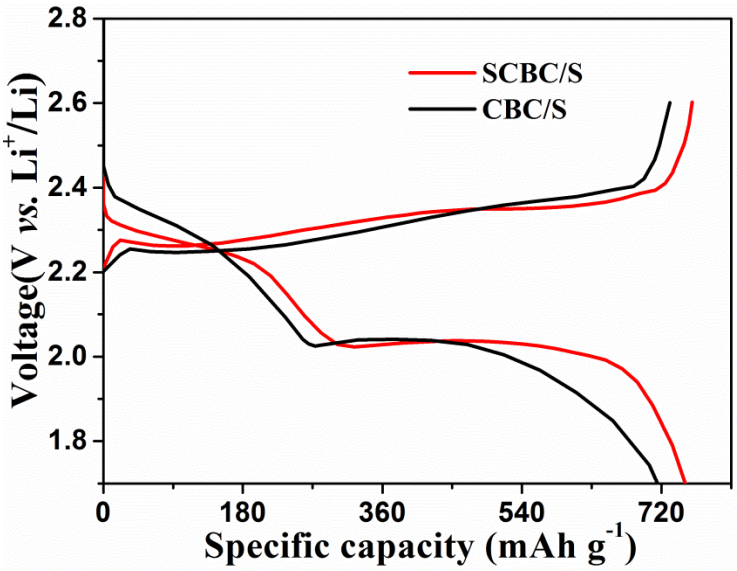

Fig. S5 Comparison of discharge/charge profiles between SCBC/S and CBC/S.

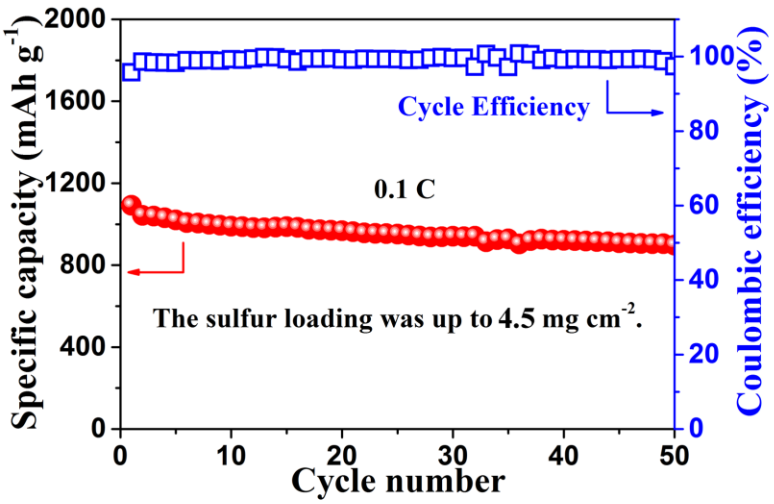

Fig. S6 Electrochemical performances. When the sulfur loading is up to 4.5 mg cm^{-2}, the cell deliverd a high initial discharge capacity of 1106 mAh g^{-1}.

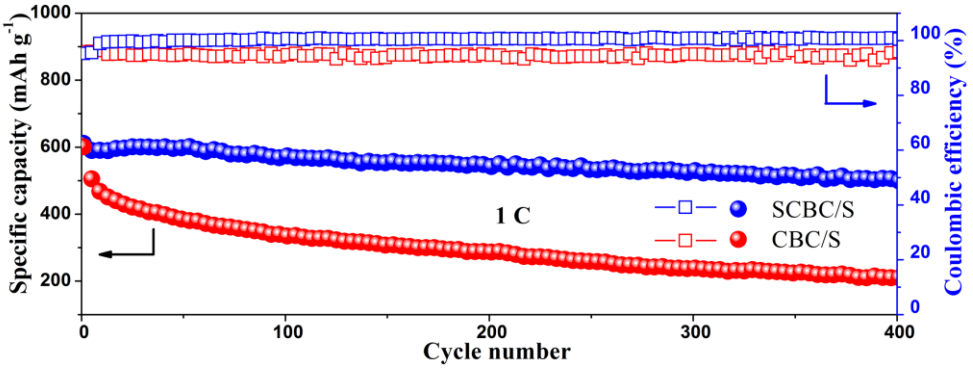

Fig. S7 The comparison of cycling performance and Coulombic efficiencies between SCBC/S cell and CBC/S cell during 400 cycles at a current rate of 1 C using 1.0 M LiTFSI in DOL/DME (1:1 by volume) without $LiNO_3$ as the electrolyte.

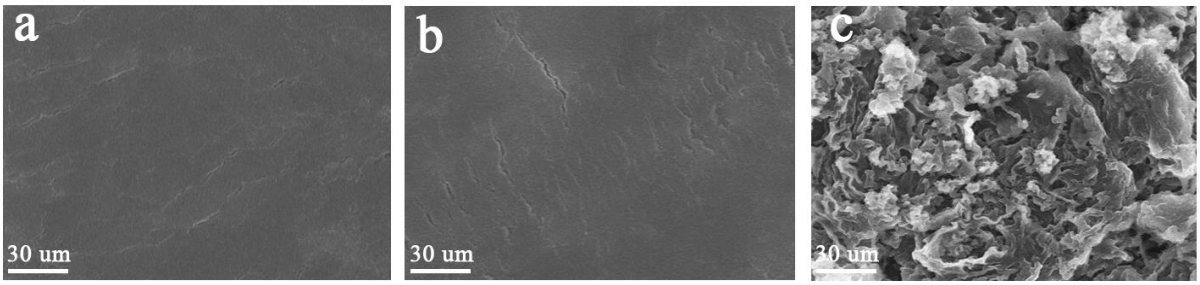

Fig. S8 SEM images of the surface of (a) the pristine anode, (b) the cycled anode of SCBC/S cell and (c) the cycled anode of CBC/S cell, respectively.

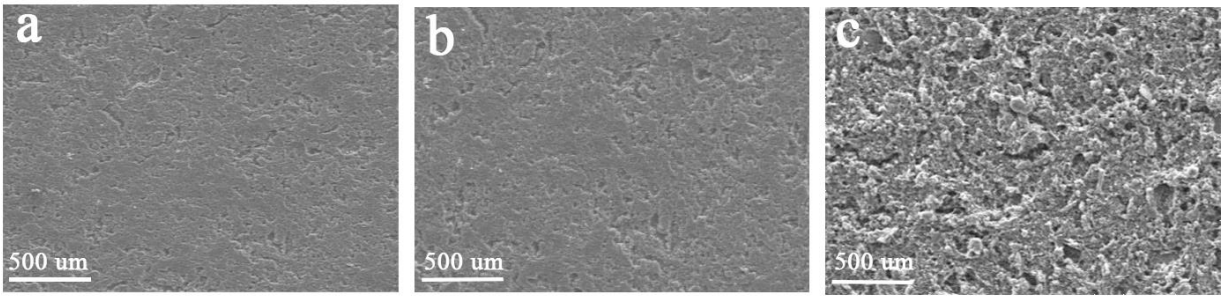

Fig. S9 SEM images of (a) the pristine cathode, (b) the cycled SCBC/S cathode and (c) the cycled CBC/S cathode, respectively.

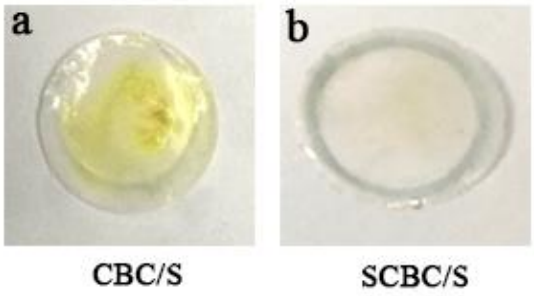

Fig. S10 Digital photos of cycled separators of (a) CBC/S cell and (b) SCBC/S cell, respectively. Both cells are disassembled after cycling tests.

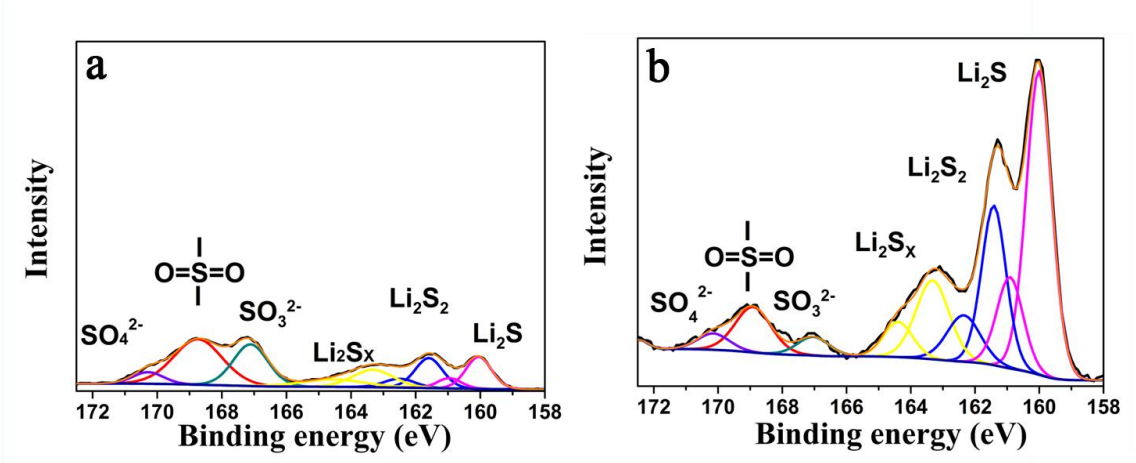

Fig. S11 High-resolution S_{2p} spectra of cycled lithium anodes using (a) SCBC/S cathode and (b) CBC/S cathode, respectively.

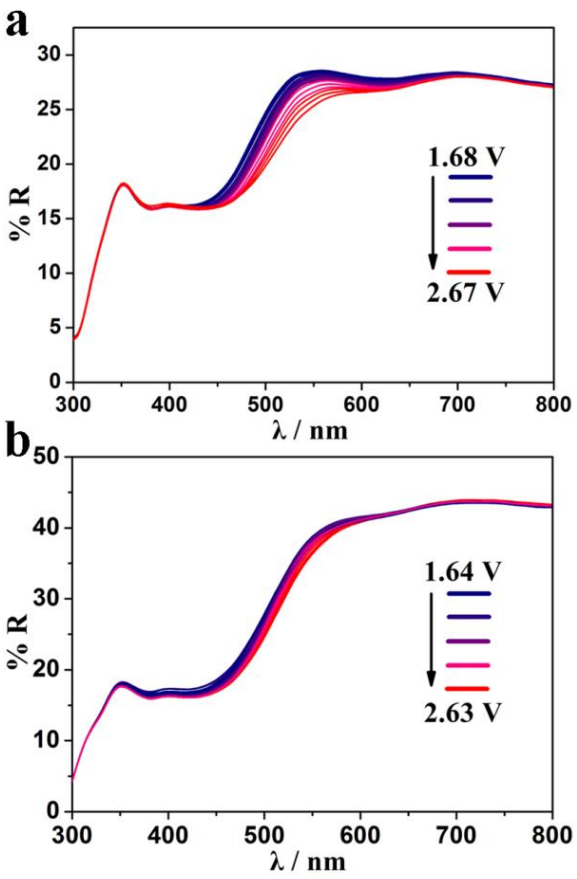

Fig. S12 Characterizations of UV/Vis spectra in cells charge processes. The comparison of UV/Vis spectra of (a) CBC/S and (b) SCBC/S in charging process. (a) The continuous shift to higher wavelengths suggests the regeneration of long-chain polysulfides. Different from (a) CBC/S, the spectra of (b) SCBC/S shift to higher wavelengths along with its discharge course.

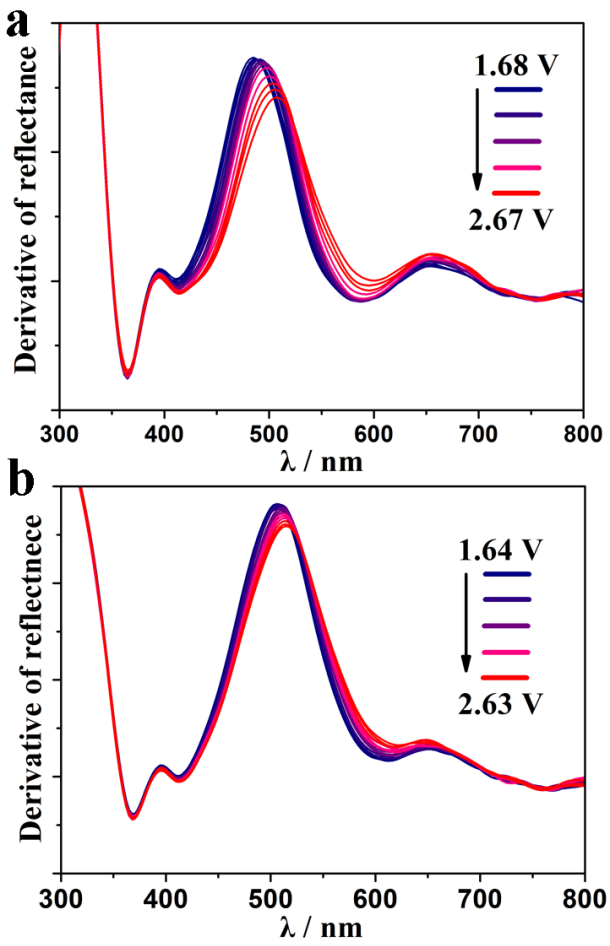

Fig. S13 Characterizations of first-order derivatives in cells charge processes. The first-order derivatives derived from UV/Vis spectra of (a) CBC/S and (b) SCBC/S cell during charging. The shift of main peaks indicates there is a change between long-chain and short-chain polysulfides in (a) CBC/S cell charging process. The derivatives of (b) SCBC/S cell keep the main peaks in 510 nm all the time.